NUMERICAL SIMULATION ON DENSE GAS-PARTICLE RISER FLOW*

ZHA Xu-dong(查旭东), FAN Jian-ren(樊建人), SUN Ping(孙平), CEN Ke-fa(岑可法)

(*Dept. of Energy Engineering, Yuquan Campus of Zhejiang University, Hangzhou, 310027, China*)

Received Dec.16, 1998; revision accepted May 18,1999

Abstract: A turbulence gas-solid model that combines Eulerian approach and Lagrangian approach is formulated, which takes inter-particle interaction into consideration on the base of kinetic theory. The numerical algorithm is included. Comparison of the model results with the experimental results of Miller and Gidaspow (1992) showed good agreement.

Key words: Eulerian approach, Lagrangian approach, inter-particle collision.
Document code: A **CLC number**: V211.1+7

INTRODUCTION

The modeling methods of gas-solid flow are known to include the Eulerian/Eulerian approach and the Eulerian/Lagrangian one. The Eulerian/Eulerian approach treats both phases as separate interpenetrating continuum, while the Eulerian/Lagrangian approach treats the gas phase as a continuum but deals with the dispersed phase by solving Lagrangian equations for the trajectory of a statistically significant amount of particles or "parcels" (groups of particles of identical size, mass, position).

The advantage of the Eulerian/Lagrangian approach is that it can yield detailed information on the dispersed phase, but may be time-consuming when applied to relatively dense particulate two-phase flow. The Eulerian/Eulerian approach has advantages of easy programming and understanding and is thought to be especially reasonable when applied to dense two-phase flow, but was found to be incompetent when confronted with two-phase flow of various particles character, such as size, density.

A really good numerical model for two-phase flow modeling must include several important interactions. For modeling of turbulence diffusion of particles, Fan et al(1997). introduced a new FSRT (Fluctuation-spectrum-random-trajectory) model into the Eulerian/Lagrangian method and achieved good result for relatively dilute two-phase jet flow. Jenkins and Savage(1983), Lun and Savage(1987) introduced a kinetic theory to account for inter-particles interaction, then global models were developed by Sinclair and Jackson(1989), Ding and Gidaspow(1990).

A major concern in this work was to set up a model using a combination of Eulerian and Lagrangian approach. At the end of this paper, we will compare our simulation results with the results of Miller and Gidaspow(1992).

MATHEMATICAL MODEL

Our model is composed of two parts: the Eulerian part and the Lagrangian one.

1. The Eulerian part

In this part, we adopted the model that was first derived on the basis of molecules kinetic theory by Ding and Gidaspow(1990), later revised by Nieuwland et al.(1996).

The basic equation is the Boltzmann equation:

$$\frac{\partial}{\partial t} + \boldsymbol{v}\frac{\partial f}{\partial x} + \frac{\partial}{\partial \boldsymbol{v}}(\boldsymbol{F}f) = \left(\frac{\partial f}{\partial t}\right)_{\text{collision}} \quad (1)$$

Mass Continuity equation:

$$\frac{\partial}{\partial t}(\varepsilon_m \rho_m) + \nabla(\varepsilon_m \rho_m \boldsymbol{v}_m) = 0 \quad (2)$$

The subscript m refers to fluid and solid in turn, representing gas phase and solid phase respectively.

* Project(59425004) supported by NSFC.

Momentum equation:

$$\frac{\partial}{\partial t}(\varepsilon_m\rho_m\boldsymbol{v}_m) + \frac{\partial}{\partial x}(\varepsilon_m\rho_m\boldsymbol{v}_m\boldsymbol{v}_m) = \beta(\boldsymbol{v}_n - \boldsymbol{v}_m) - \varepsilon_m\frac{\partial P}{\partial x} + \frac{\partial \tau_m}{\partial x} + \varepsilon_m\rho_m\boldsymbol{g} \quad (3)$$

In Eq.(3) above, the subscript n is the opposite of m and refers to s (solid), f (fluid) in turn, representing the solid phase and gas phase respectively.

Chapman and Cowling(1970) recommended progression approximation to the velocity distribution function $f(v, x, m, t)$ in gas kinetic theory, so as to integrate the Boltzmann equation. When deriving the momentum equation of the solid-phase, to integrate terms such as $\int f\rho\,\overline{VV}dv$ or collision source term $\left(\frac{\partial f}{\partial t}\right)_{\text{collisison}}$, Ding and Gidaspow(1990) adopted the zero-order solution to the velocity distribution function, or Maxwell distribution function. Chapman and Cowling (1970) pointed out that for slightly not uniform compact gas, on which the derivation of the solid-phase equation is based, the first-order solution to the velocity distribution function is more reasonable. In this work, we use the results of Nieuwland who revised the gas kinetic theory model by integration with the first-order solution of the velocity distribution function.

For the gas phase:

$$\tau_s = -\frac{2}{3}\mu_f \mathrm{div}\,\boldsymbol{v}_f\delta_{ij} + 2\mu_f\varepsilon_{ij} \quad (4)$$

For the solid phase:

$$\tau_s = \left[-p_s + \left(\zeta_s - \frac{2}{3}\mu_s \mathrm{div}\,\boldsymbol{v}_s\right)\right]\delta_{ij} + 2\mu_s\varepsilon_{ij}$$

$$= -\left\{p_s^c + p_s^k) + \left[\zeta_s - \frac{2}{3}(\mu_s^c + \mu_s^k)\mathrm{div}\,\boldsymbol{v}_s\right]\right\}$$

$$\delta_{ij} + 2(\mu_s^k + \mu_s^c)\varepsilon_{ij} \quad (5)$$

Where,

$$p_s = p_s^k + p_s^c \quad (6)$$

is the "solid pressure" composed of a kinetic part and a collision part.

$$p_s^c = 2\varepsilon_s^2\rho_p g_0(1 + e)T_s \quad (7)$$

$$p_s^k = \varepsilon_s\rho_p T_s \quad (8)$$

where, $\frac{2}{3}T_m = \frac{1}{2}\overline{VV}$ (9)

T_m is the pseudo-temperature (m means gas, solid in turn) and V is Brown moving velocity of gas molecules for gas, and of particles for solid. For gas T_f is the real thermal temperature, while for the solid-phase T_s reflects only Brown moving fluctuation tendency but not its real temperature which is the kinetic fluctuation energy of the molecules inside the particle. So, it is called "pseudo-thermal temperature" for solid-phase.

Solid bulk viscosity coefficient is:

$$\zeta_s = \frac{4}{3}\varepsilon_s\rho_s d_p g_0(1 + e)\sqrt{\frac{T_s}{\pi}} \quad (10)$$

Solid viscosity coefficient is:

$$\mu_s = \mu_s^c + \mu_s^k\frac{\left(1 + \frac{8}{5}\frac{(1+e)}{2}\varepsilon_s g_0\right)\left(1 + \frac{8}{5}\varepsilon_s g_0\right)}{\varepsilon_s g_0} \quad (11)$$

$$\mu_s^k = 1.01600\frac{5}{16}\frac{m_p}{d_p^2}\sqrt{\frac{T_s}{\pi}} \quad (12)$$

$$\mu_s^c = \frac{4}{5}\varepsilon_s\rho_s d_p g_0(1 + e)\sqrt{\frac{T_s}{\pi}} \quad (13)$$

Fluctuation equation of solid

The pseudo thermal energy equation of the solid phase:

$$\frac{3}{2}\left[\frac{\partial}{\partial t}(\varepsilon_s\rho_s T_s) + \frac{\partial}{\partial x}(\varepsilon_s\rho_s T_s\boldsymbol{v}_s)\right] = -(P_s^c + P_s^k)\frac{\partial \boldsymbol{v}}{\partial x} - \frac{\partial}{\partial x}(q_s^k + q_s^c) + \gamma + \beta(\overline{V_f V_s} - 3T_s) \quad (14)$$

in which,

$$q^k = -\frac{\varepsilon_k\lambda^k}{\varepsilon_s g}\left(1 + \frac{12}{5}\varepsilon_s g_0\right)\frac{\partial T_s}{\partial x} \quad (15)$$

$$\lambda_s^k = 1.02513\frac{75}{64}\frac{m}{d_p^2}\sqrt{\frac{T_s}{\pi}} \quad (16)$$

$$q^c = -\varepsilon_s\lambda^c\frac{\partial T}{\partial x} - \frac{u^k}{g_0}\frac{6(1 + e)}{5}$$

$$\varepsilon_s g_0\left(1 + \frac{12}{5}\varepsilon_s g_0\right)\frac{\partial T_s}{\partial x} \quad (17)$$

$$\lambda^c = 2\varepsilon_s\rho_s d_p g_0(1 + e)\sqrt{\frac{T_s}{\pi}} \quad (18)$$

$$\gamma = -3(1-e^2)\varepsilon_s^2\rho_s g_0 \nabla \cdot \boldsymbol{v}_s \tag{19}$$

$$\overline{V_f V_s} = \frac{4d_p\beta(u_f - u_s)^2}{\pi^{1/2}\rho_s \upsilon_v T_s^{1/2}} \tag{20}$$

as recommended by Louge et al(1991).

The drag coefficient is the one introduced by Ding and Gidaspow(1990).

$$\varepsilon_s < 0.8 \quad \beta = 150\frac{(1-\varepsilon)^2\mu_G}{\varepsilon d_p} + 1.75\frac{\rho_G(1-\varepsilon)\,|\,\boldsymbol{u}_G - \boldsymbol{v}_P\,|}{d_p} \tag{21}$$

$$\varepsilon_s \geq 0.8 \quad \beta = \frac{3}{4}C_d\frac{\varepsilon\theta\rho_G\,|\,\boldsymbol{u}_G - \boldsymbol{v}_P\,|}{d_p}\varepsilon^{-2.65} \tag{22}$$

where, for

$$\mathrm{Re}_p < 1000,\ C_d = \frac{24}{\mathrm{Re}_p}[1 + 0.15(\mathrm{Re}_p)^{0.678}] \tag{23}$$

$$\mathrm{Re}_p \geq 1000,\ C_p = 0.44 \tag{24}$$

Reynolds number of solid is:

$$\mathrm{Re}_p = \frac{\varepsilon\rho_G(1-\varepsilon)\,|\,\boldsymbol{u}_G - \boldsymbol{v}_P\,|}{\mu_G} \tag{25}$$

g_0 in the equations above is a radial distribution function used account for the influence of the solid concentration on the collision frequency. In this work, we adopted the expression recommended by Ma and Ahamidi(1986).

$$g_0 = \frac{1 + 2.5\varepsilon + 4.5904(\varepsilon)^2 + 4.515439(\varepsilon)^3}{\left[1 - \left(\frac{\varepsilon}{\varepsilon_{\text{packing}}}\right)^3\right]^{0.678021}} \tag{26}$$

When the volume fraction of the solid phase is reduced to zero, g_0 is reduced to zero. The equations above are for gas only; at the packing limit $\varepsilon_{\text{packing}} = 0.64356$, g_0 will be infinity. That will make the particle in the two-phase flow immovable.

Gas turbulence equation

In this paper we introduced a revised $k-\varepsilon$ two-equation model inspired by Bolio et al (1995).

$$\nabla \cdot (\rho_f \boldsymbol{u}_f \varepsilon_f k) = \nabla \cdot \left[\left(\mu_m + \frac{\mu_f}{\sigma_k}\right)\nabla \cdot (\varepsilon_f k)\right] + G - \rho_f\varepsilon_f E - \beta(2k - \overline{V_f V_s}) \tag{27}$$

in which G is the fluctuation production term, briefly written as:

$$G = \mu_f(\nabla \cdot \boldsymbol{u}_f)^2 \tag{28}$$

$$\nabla \cdot (\rho_f \boldsymbol{u}_f \varepsilon_f E) = \nabla \cdot \left[\left(\mu_m + \frac{\mu_f}{\sigma_E}\right)\nabla \cdot (\varepsilon_f E)\right] + c_1 G\frac{E}{k}\varepsilon_f E - c_2 G\varepsilon_f\frac{E^2}{k} - c_3\beta(2k - \overline{V_f V_s})\frac{E}{k} \tag{29}$$

2. The Lagrangian part

We try to combine the gas phase and solid phase together in the same equations because we want to emphasize there is compatibility between gas molecules and particles. This was useful in our setting up the mathematical model of the Lagrangian part. In fact, in the original equation of motion of a single particle or "parcel"(a group of particles of identical size, velocity and position), the momentum exchange between the two phases is due to the collisions between gas molecules and particles. If we consider the solid-phase as a different kind of fluid that exists simultaneously with gas fluid in every point of the controlled volume, as we do in Eulerian/Eulerian models, there are two kinds of continua: "gas fluid" and "solid fluid", both having the character of continuum such as shear viscosity, bulk viscosity, pressure, etc.; those of the "solid fluid" reflect the kinetics and collision mechanism between particles. Then if one single particle or "parcel" is traced in the mixture of the two kinds of continua, force will be exerted on it from both "fluids". Drag force and pressure force from the "gas fluid" are due to collisions between gas molecules and particles, while drag force and pressure force from the "solid fluid" are due to collisions between the whole particles of the "solid fluid" and particles in the dispersed "parcel". If all dispersed "particles" or "parcels" are traced in this way finally, then put back into the Eulerian/Eulerian equations to get their "fluid character" again, we will account for inter-phase interaction and inter-particle interaction in every detail, even with highly dispersed particle size or density distribution. That is the base on which we set up our new model.

The new equation of motion of particles and "parcels" is:

$$m_p \frac{du_p}{dx} = \frac{dP}{dx} - \frac{dp_s}{dx} + \beta_f(\boldsymbol{u}_f - \boldsymbol{u}_p) + F_{sp} + m_p\boldsymbol{g} \quad (30)$$

The momentum equation of solid continuum is the sum of the equations of motion of all particles.

To model the new drag force of "solid fluid" on dispersed "particle", we introduce:

$$F_{sp} = (\boldsymbol{u}_f - \boldsymbol{u}_p)/\tau_c \quad (31)$$

where τ_c is the mean inter-particle collision time interval.

$$\tau_c = \frac{1}{\frac{6}{d_p}\varepsilon_s g\sqrt{\frac{32}{3\pi}T_s}} \quad (32)$$

In Eq. (27), when solid volume fraction ε_s is zero, the second and fourth term at the right of the equation will be zero; when ε_s is the maximum (for round stochastic distribution particle, it is 0.64356), the second and fourth term at the right of the equation will be infinity.

In this part, the turbulence diffusion of particles is considered in such a way as recommended by Fan et al(1997).

The instantaneous gas phase velocity is:

$$u_f = U_f = u'_f \quad (33)$$

where, U_f is the average velocity obtained from the mean velocity field. The fluctuating velocity in an eddy is simulated by a random Fourier series:

$$u'_f = \sum_{n=1}^{n=10} R_1 U_m \cos(\bar{\omega}_n t - R_2\alpha) \quad (34)$$

in which, R_1, R_2 are random numbers between zero and unity, α is the initial fluctuating phase, $\bar{\omega}_n$ is sampled from a Gaussian distribution with a standard deviation of unity. For incompressible, isotropic turbulence flow field, the fluctuation amplitude is:

$$U_m = \left(\int_0^{\infty} E(K)\,dK\right)^{1/2} \quad (35)$$

$E(K)$ is the energy spectrum, K is the wave number.

$$E(K) = 16\left(\frac{2}{\pi}\right)^{1/2} K^4 e^{-2K^2} \quad (36)$$

SIMULATION ALGORITHMS

The main purpose of this work was to formulate a new method that will have the advantages of both the Eulerian approach and the Lagrangian approach.

We first rewrite our basic equations in order to use our CEL approach.

The gas-phase momentum equation:

$$\frac{\partial}{\partial t}(\varepsilon_f\rho_f\boldsymbol{v}_f) + \frac{\partial}{\partial x}(\varepsilon_f\rho_f\boldsymbol{v}_f\boldsymbol{v}_f) = M_{\text{interphase}} - \varepsilon_f\frac{\partial P}{\partial x} + \varepsilon_f\rho_f\boldsymbol{g} + \frac{\partial \tau_f}{\partial x} \quad (37)$$

The solid-phase momentum equation:

$$\frac{\partial}{\partial t}(\varepsilon_s\rho_s\boldsymbol{v}_s) + \frac{\partial}{\partial x}(\varepsilon_s\rho_s\boldsymbol{v}_s\boldsymbol{v}_s) = M_{\text{interphase}} - \varepsilon_s\frac{\partial P}{\partial x} + \varepsilon_s\rho_s\boldsymbol{g} + \frac{\partial \tau_s}{\partial x} \quad (38)$$

The procedure of our simulation method is as follows.

1. Set an initial field of ε_s, $\boldsymbol{u}_f$, $\boldsymbol{v}_f$, $\boldsymbol{u}_s$, $\boldsymbol{v}_s$, k, e separately representing solid volume fraction, gas velocity of x, y coordinate, solid velocity of x, y coordinate, gas fluctuation energy and dissipation.

2. Solve Eqs. (37), (38) and gas turbulence equations to get ε, $\boldsymbol{u}_s$, $\boldsymbol{v}_s$, $\boldsymbol{u}_f$, $\boldsymbol{v}_f$, k, e as the Eulerian part.

3. Solve Eq. (14) to get "solid pseudo thermal energy", then solve for "solid viscosity", "solid pressure" "solid bulk viscosity", "solid effective viscosity" in the corresponding equation.

4. Put the above "solid fluid characteristics" parameters into Eq. (30); then trace the statistically large number of "parcels" until they leave the computational volume. Then the statistically calculate source term can be obtained by summing up all "parcels" on every cell:

$$S_{p,i} = \sum_n m_p(\boldsymbol{u}_{p,\text{in}} - \boldsymbol{u}_{p,\text{out}}) \quad (39)$$

In this part, the turbulent diffusion of particles is taken into consideration.

5. Put back the "source term" in the Eulerian equation, then repeat step 2. again until convergence is obtained.

In fact, the "source term" is composed of two parts:

$$S_{p,i} = M_{\text{gas-particle}} + M_{\text{solid-particle}} \quad (40)$$

The "source term" considers inter-phase interaction of "parcels and gas" and inter-particles interaction.

After taking account of all particles or "parcels" and after convergence is obtained, theoretically:

$$\sum M_{\text{gas-particle}} = \beta(\boldsymbol{u}_f - \boldsymbol{u}_s) \quad (41)$$

$$\sum M_{\text{solid-particle}} = 0 \quad (41)$$

In the end, after the convergence has been obtained, the mean velocity and mean solid fraction on a cell given by the dispersed particle motion equation will be nearly the same as that given by the continuum equation.

Near wall, gas velocity and turbulence kinetic energy are zero. For the solid-phase, we adopted the condition recommended by Sinclair and Jackson(1989).

For momentum:

$$-\varepsilon_s \mu_s \frac{\partial v_y}{\partial x} = \frac{\rho_s \pi v_y \Phi \sqrt{T_s}}{2\sqrt{3}\left[\frac{\varepsilon_{\text{packing}}}{\varepsilon_s} - \left(\frac{\varepsilon_{\text{packing}}}{\varepsilon_s}\right)^{2/3}\right]} \quad (43)$$

For "pseudo temperature":

$$\left(-\lambda \frac{\partial T_s}{\partial x}\right) = \frac{-\rho_s \pi v_y \Phi \sqrt{T_s}}{2\sqrt{3}\left[\frac{\varepsilon_{\text{packing}}}{\varepsilon_s} - \left(\frac{\varepsilon_{\text{packing}}}{\varepsilon_s}\right)^{2/3}\right]} + \frac{\sqrt{3}\rho_s \pi (1 - e_w) T_s^{2/3}}{4\left[\frac{\varepsilon_{\text{packing}}}{\varepsilon_s} - \left(\frac{\varepsilon_{\text{packing}}}{\varepsilon_s}\right)^{2/3}\right]} \quad (44)$$

in which

$$\lambda_s = \lambda_s^c + \lambda_s^k \frac{\left(1 + \frac{12(1+e)}{5\quad 2}\varepsilon_s g_0\right)\left(1 + \frac{12}{5}\varepsilon_s g_0\right)}{\varepsilon_s g_0} \quad (45)$$

In this paper, the inter-particle collision restitution coefficient e is 0.985, inter-particle collision restitution coefficient e_w is 0.92, specularity factor Φ is 0.5.

RESULT AND DISCUSSION

The results presented here were obtained using 150 × 40 non-uniform nodes to cover the two-dimension flow domain. No less than 10 000 particle parcels were considered.

We compared our numerical prediction with the experimental results of Miller and Gidaspow (1992) who measured the overall characteristic of dense gas-solid flow in riser. In order to cover as much as ground as possible in our discussion, we chose six different situations for comparison and discussion even though there were no experiment results available for all cases; that is, cases with inlet solid flux being 12.0 kg/($m^2 \cdot s$) and 20.4 kg/($m^2 \cdot s$), superficial gas velocity being 2.89 m/s and 3.48 m/s, and location being 1.86 m and 4.18 m away from inlet, respectively.

At the inlet, uniform particle velocity was deduced from the needed inlet solid mass flux, a constant solid volume fraction of 0.1 was taken, "pseudo temperature" was set to be zero. At first, identical 75 μm particles with density of 1600 kg/m^3 were used, then three groups of 40 μm, 70 μm, 100 μm particles with initial volume fraction of 0.033, 0.033, 0.033 were used.

Fig. 1(a) on the velocities of both phases shows that due to the free velocity wall condition for the solid-phase, downwards movement of particles is predicted (also found in the experiment of Miller and Gidaspow), which implies the test height in this case was in "dilute region" composed of "core region", and "annular region" in FBC technology. The gas velocity was higher than solid velocity. Velocities of both phases maximized in the core, and decayed towards the wall due to the wall effect. The turbulent fluctuation energy is shown in Fig. 1(b); the turbulent fluctuation energy is represented by turbulence intensity for gas-phase while it is the pseudo temperature for solid-phase. The fluctuation energy of the gas phase was found to be higher than that of the solid phase because the gas-phase was the carrier phase. The relatively stronger inter-particles collision in the core decreases the solid phase fluctuation energy. Toward the wall, it increases due to the gradually dominating kinetic mechanism. The competition between the kinetic transport and inter-particles collision is the mechanism of inter-particle interaction. Gas-phase turbulence fluctuation energy is also reduced by the increased solid loading ratio. Fig. 1(c) shows that the prediction is in good agreement with the experiment result even though somewhat overestimated in the core, probably because of the difference between the inlet condition used in simulation and that used in the experiment. And due to the asymmetry in the experiment, it is also underestimated at the right side. The somewhat higher value of volume fraction near the wall is due to the higher downward velocity from the above annular region. In the core, particles are accelerated upwards at relatively high velocity. Fig. 1(d) also shows the results, which is not reported in the experiment of Miller and Gidaspow(1992).

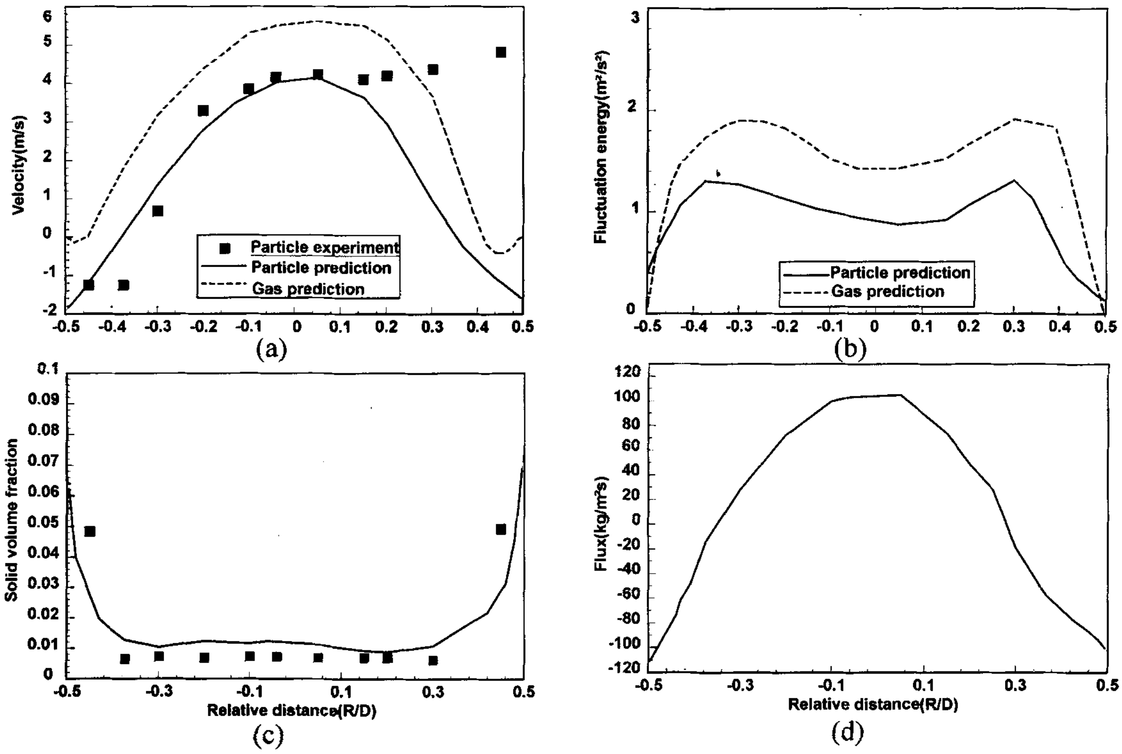

Fig. 1 Profiles of velocity (a); fluctuation energy (b); solid volume fraction (c); solid flux (d) for inlet flux = 12.0 kg/m^2·s, inlet superficial gas velocity 2.89 m/s, 1.86 m away from the inlet.

Comparison with Fig. 2 shows that its profiles of velocities are similar to those of Fig. 1(a), except that gas velocities in Fig. 2(a) are somewhat steeper and a marked downwards flow is predicted. The flattened velocity profile is supposed to be due to the decrease of solid flux as shown in Fig. 2(d). At the same time, higher slip velocity is also observed due to the relatively dilute concentration. Fluctuation of gas is higher than that at the position 1.86 m away from the inlet. Difference between fluctuation of the two phases is more marked; the fluctuation energy of solid is flattened and lower due to the dilute mass flux.

Fig. 3(a), (b) show that the slip velocity and fluctuation difference of solid flux (20.4 kg/m^2·s) are all lower than that of solid flux (12.0 kg/m^2·s), which is due to the inter-phase momentum and energy exchange. Moreover, stronger random collisions also steepened the profile of the solid energy distribution. Because of the increased solid inlet flux, both solid volume fraction and solid flux are higher when compared with that in Fig. 1 as shown in Fig 3(c), (d). The same reason can be used to explain the related differences between Fig. 2 and Fig. 4.

In Fig. 5, the superficial gas velocity is raised to 3.48 m/s. Compared to Fig. 3, one can find that the gas velocity is raised too, and raised too is the slip velocity due to the inertia effect of solid. No downward velocity is found in the profiles of gas velocity. Because of the raised Reynolds number, the phase exchange increases, and phase fluctuation is higher. But since

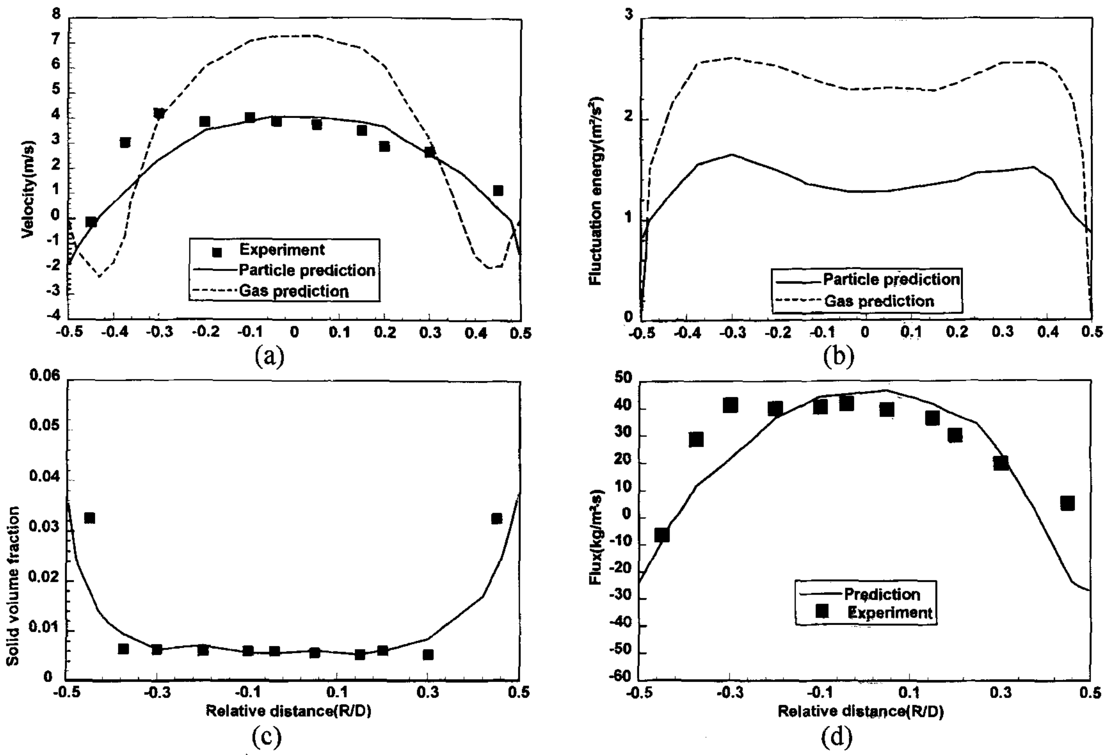

Fig.2 **Profiles of velocity (a); fluctuation energy (b); solid volume fraction (c); solid flux (d) for inlet flux = 12.0 kg/m^2·s, inlet superficial gas velocity 2.89 m/s, 4.18 m away from the inlet.**

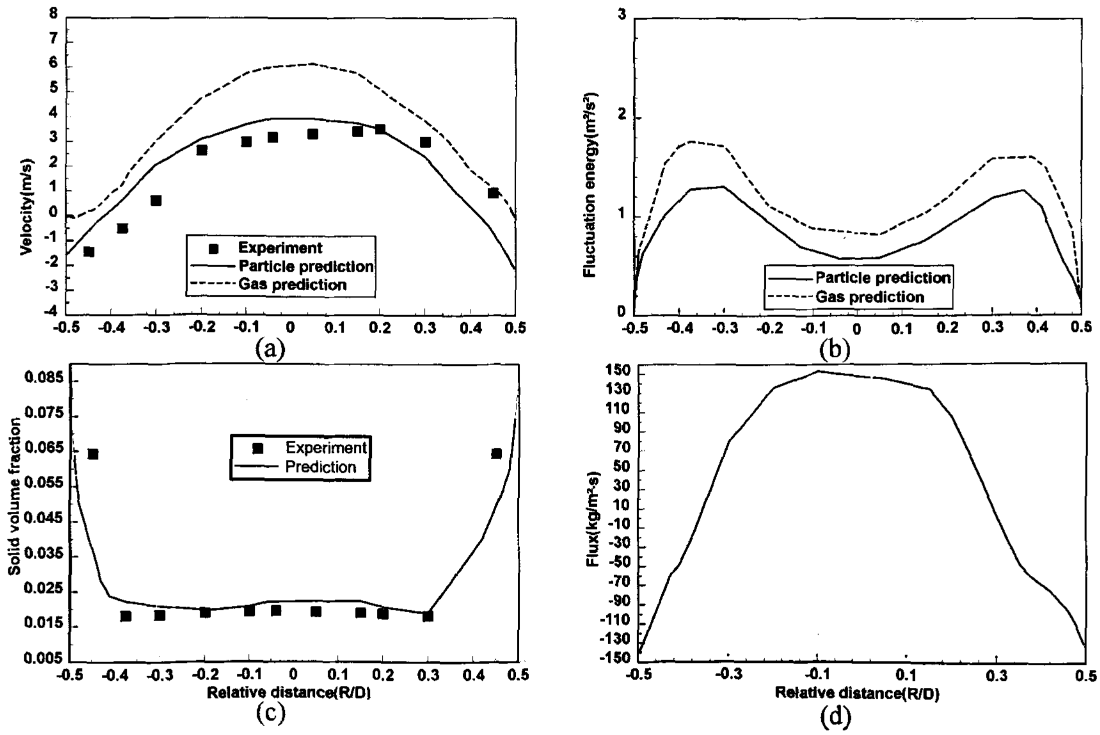

Fig.3 **Profiles of velocity (a); fluctuation energy (b); solid volume fraction (c); solid flux (d) for inlet flux = 20.4 kg/m^2·s, inlet superficial gas velocity 2.89 m/s, 1.86 m away from the inlet.**

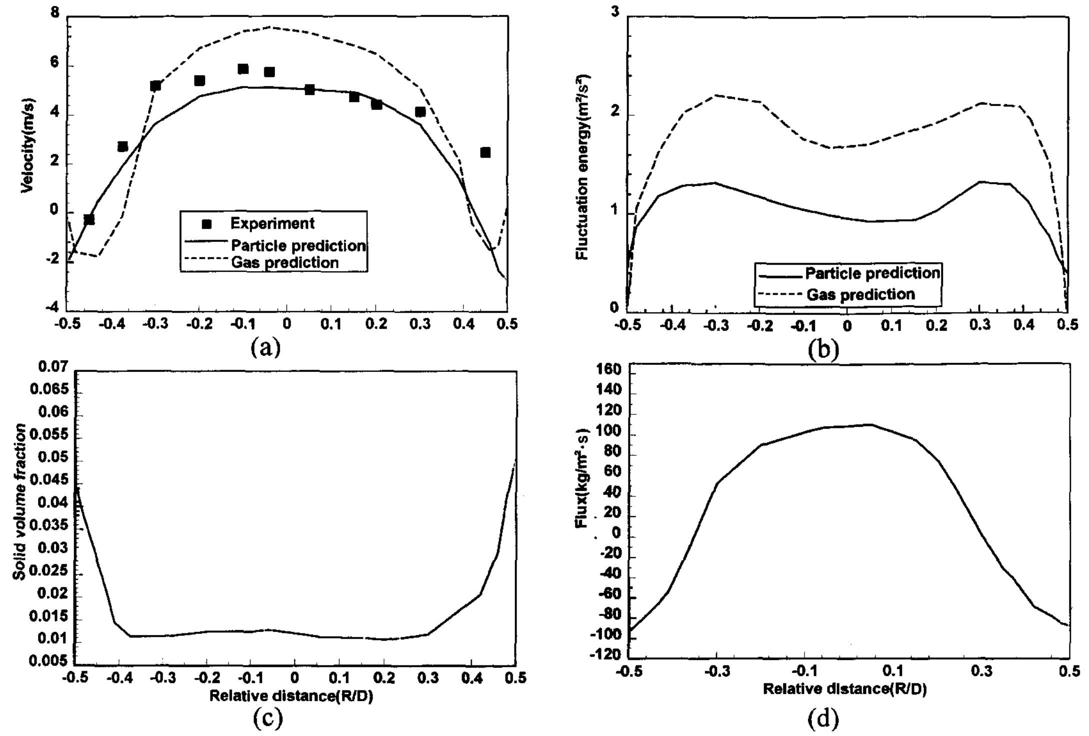

Fig.4 Profiles of velocity (a); fluctuation energy (b); solid volume fraction (c); solid flux (d) for inlet flux = 20.4 kg/m^2·s, inlet superficial gas velocity 2.89 m/s, 4.18 m away from the inlet.

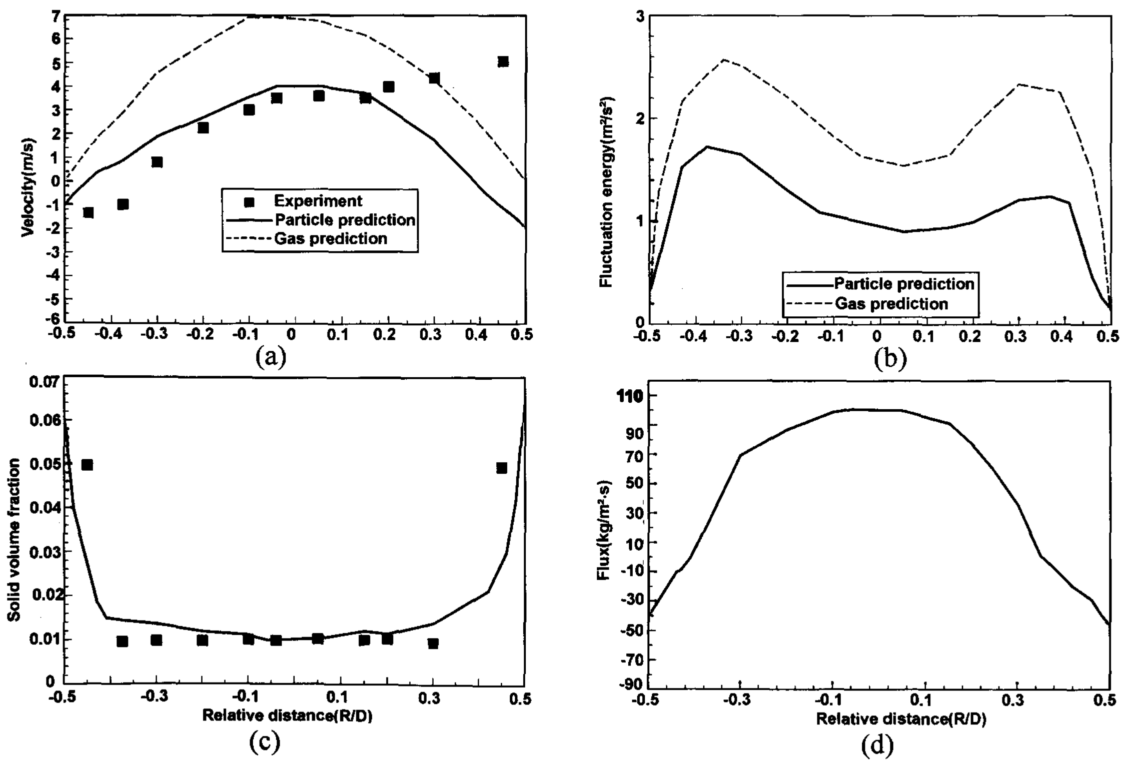

Fig.5 Profiles of velocity (a); fluctuation energy (b); solid volume fraction (c); solid flux for inlet flux = 20.4 kg/m^2·s(d), inlet superficial gas velocity 3.48 m/s, 1.86 m away from the inlet.

more particles are taken upwards, the resulting solid volume fraction in Fig. 5(c) is lower than that in Fig. 3(c). The same reason also explains why the solid flux is decreased is Fig. 3(d) and Fig. 5(d). These conclusions are all in agreement with the experimental results of Ding and Gidaspow(1990). In Fig. 6, due to the raised height, more downward gas and particles are predicted as shown in the profiles of velocity and solid flux. Lower and flattened solid fluctuation profile and lower solid volume fraction are shown.

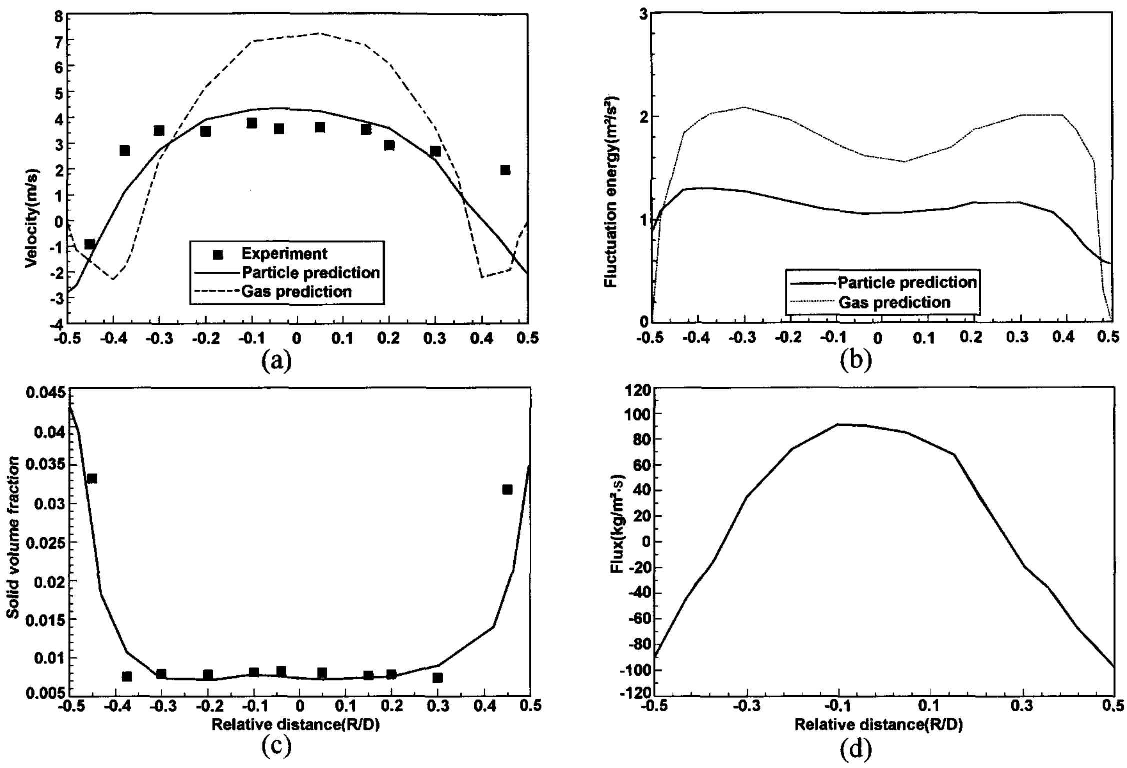

Fig. 6 Profiles of velocity (a); fluctuation energy (b); solid volume fraction (c); solid flux (d) for inlet flux = 20.4 kg/m^2·s, inlet superficial gas velocity 3.48 m/s, 4.18 m away from the inlet.

We can see that the above results agree reasonably well with the experiment results, esp. at the height of $h = 4.18$ m, because of the well-developed flow there.

In the original Eulerian/Eulerian approach, only the mean identical size particles can be considered. Our new model is more convenient and can take into account a wide range of particle characteristics, e.g. varied size.

Fig. 7 shows velocities of varied size particles

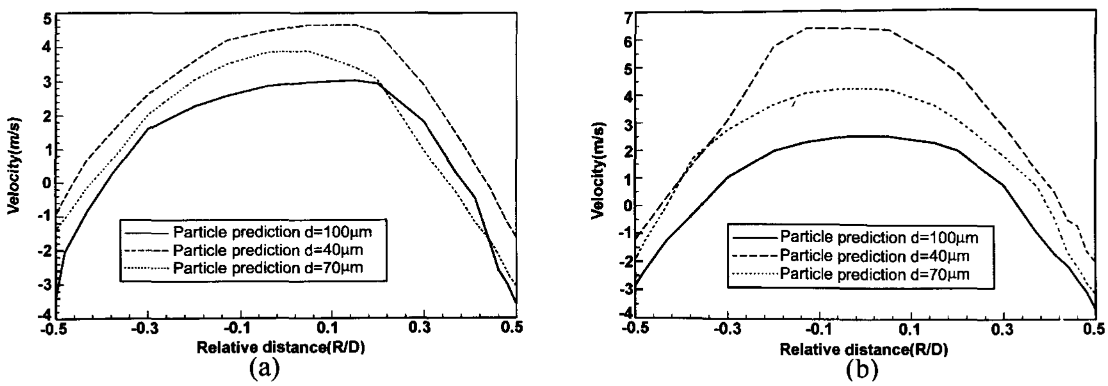

Fig. 7 Profiles of solid velocity (a) at 1.86 m away from the inlet; (b) 4.18 m away from the inlet; total flux = 20.4 kg/m^2·s, inlet superficial gas velocity 3.48 m/s.

at the same position. One can see that at lower position, due to the dominating effect of the inlet condition, difference between the three groups is not marked, but raised to the height of 4.18 m, difference is more marked due to the different acceleration process.

Fig. 8 shows the solid volume fraction of different particles. Larger particles need more drag force to accelerate so they are almost left behind and so, have extremely lower concentration at height of 4.18 m.

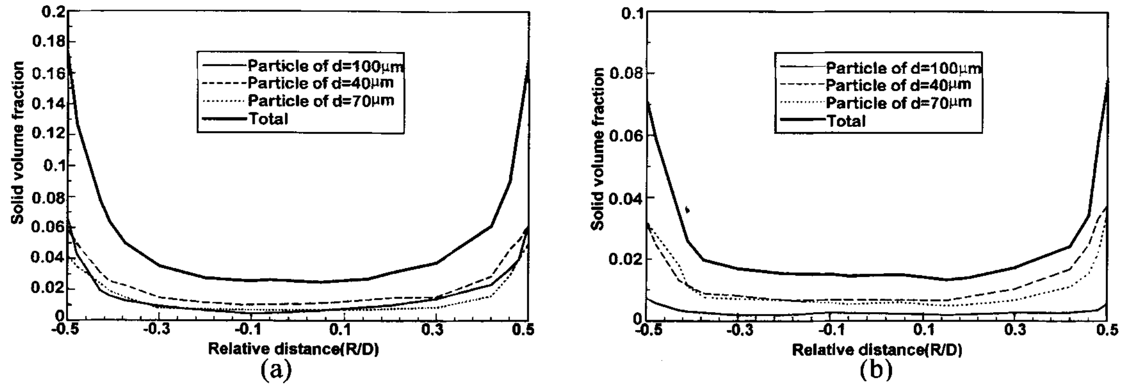

Fig.8 Profiles of solid volume fraction (a) at 1.86 m away from the inlet; (b) 4.18 m away from the inlet; total flux = 20.4 kg/m^2·s, inlet superficial gas velocity 3.48 m/s.

CONCLUSION

In this paper, we set up a new model that combines Eulerian and Lagriangian approach so as to make best use of the advantages of both. In our model, inter-particle interaction is treated on the base of kinetic theory, so that it can be applied to relatively dense particulate two-phase flow. In the end, for dense gas-solid upward flow in riser, good agreement was reached between the prediction results and the experimental results of Ding and Gidaspow(1990).

References

Bolio, E.J., Yasuna, J.A., Sinclair, J.L., 1995. Dilute turbulent gas-solid flow in riser with particle-particle interaction. *AIChE. Journal*, **6**: 1375 – 1388.

Chapman, A., Cowling, T.G., 1970. The mathematical Theory of Non-Uniform Gases. 3rd. ed., Cambridge Univ. Press, Cambridge.

Ding, J., Gidaspow, D., 1990. A bubbling fluidization model using kinetic theory of granular flow. *AIChE. Journal*. **4**: 523 – 538.

Fan, J.R., Zhang, X.Y., Chen, L.H. et al., 1997. New stochastic particle dispersion modeling of a turbulent particle-laden round jet. *the Chemical Engineering Journal*. **66**: 207 – 215.

Jenkins, J.T., Savage, S.B., 1983. A theory for the rapid flow of identical, smooth nearly elastic spherical particles. *J. Fluids Mech*. **130**: 187 – 199.

Lounge, M.Y, Mastorakos, E., Jenkins, J.T., 1991. The role of particle collisions in pneumatic transport. *J. Fluids Mech*., **231**: 345 – 359.

Lun, C.K., Savage S.B., 1987. A simple kinetic theory granular flow of rough, inelastic, spherical particles. *J. Applied Mech*. **54**: 47 – 53.

Ma, D., Ahamadi, G., 1986. An equation of state for dense rigid sphere gases. *J. Chem. Pays*. **84**: 3449 – 3450.

Miller, A., Gidaspow, D., 1992. Dense, vertical gas-solid flow in a pipe. *AIChE. J*. **11**: 1801 – 1815.

Nieuwland, J.J., Annaland, S. M. van, Kuipers J.A., et al., 1996. Hydrodynamics modeling of gas/particle flows in riser reactors. *AIChE. J*. **6**: 1569 – 1582.

Sinclair, J.L., Jackson, R., 1989. Gas-particle flow in a vertical pipe with particle-particle interaction. *AIChE. Journal*, **9**: 1473 – 1487.